Available online at www.eccomasproceedia.org
Eccomas Proceedia COMPDYN (2019) 5741-5755

ECCOMAS
Proceedia

COMPDYN 2019
7th ECCOMAS Thematic Conference on
Computational Methods in Structural Dynamics and Earthquake Engineering
M. Papadrakakis, M. Fragiadakis (eds.)
Crete, Greece, 24–26 June 2019

WIND PERFORMANCE ASSESMENT OF TELECOMMUNICATION TOWERS: A CASE STUDY IN GREECE

Dimitrios V. Bilionis[1], **Dimitrios Vamvatsikos**[2]

[1] PhD Candidate
Institute of Steel Structures, School of Civil Engineering, National Technical University of Athens
Zografou Campus, Iroon Polytechneiou 9, 15780 Zografou, Athens, Greece
e-mail: dimbilionis@central.ntua.gr

[2] Assistant Professor
Institute of Steel Structures, School of Civil Engineering, National Technical University of Athens
Zografou Campus, Iroon Polytechneiou 9, 15780 Zografou, Athens, Greece
e-mail: divamva@mail.ntua.gr

Abstract

Steel lattice towers are widely used by telecommunication companies to install radiowave dish antennas for the expansion of their network. They are tall highly-optimized structures for which severe weather conditions including low temperatures, snow and high winds are the governing loading conditions. Specifically, high winds in combination with accumulated ice on the members of the structure and the dishes are the leading causes of collapse. The focus is on a standardized model of a telecommunication tower used by major telecommunication companies in Greece. The model is designed according to European Standards for areas located at distances lower than 10km from the coastline. The tower is 48 meters tall, having a square cross-section whose dimensions generally reduce with height and it employs channel and angle steel sections. Non-linear dynamic analyses were performed in order to estimate the fragility of the structure to wind and/or icing conditions. Wind loads were simulated via a 3D wind field fully capturing the spatial and temporal variation of wind speed over the entire profile of the tower for different reference values of wind speed. The impact of ice was assessed by considering a range of different uniformly thick layers of ice that increase the weight as well as the cross-section area of all members and dishes. The ultimate goal of this work is to provide the fragility functions for every potential combination of wind and icing conditions that could be observed during the service life of the structure. Thus, by incorporating the corresponding climactic hazard surfaces, the risk of tower collapse is estimated over its entire projected lifetime, offering a useful decision support tool to telecommunication companies regarding the need to replace or upgrade their existing tower network on a case-by-case basis.

Keywords: Telecommunication Tower, Steel Lattice Structure, Wind, Ice, Fragility

ISSN:2623-3347
Peer-review under responsibility of the organizing committee of COMPDYN 2019.
doi: 10.7712/120119.7342.19629

1 INTRODUCTION

Rapid advances in data transmission technology and telecommunications introduce new engineering challenges affecting not only the electromechanical components (e.g. microwave dishes) of a telecommunication network but also the supporting structures. Supporting structures are usually tall highly-optimized steel lattice towers. These structures are vulnerable to weather hazards with wind, low temperatures and corresponding ice accretion being the most critical loading conditions.

Relevant experience, especially from power transmission networks, has shown that storm events may lead to significant damage of steel lattice towers of a network resulting in total collapses with adverse impact for the whole operation of the network, in most of the times associated with considerable long downtime in service and significant economic loss. The above effect of strong winds is further enhanced when ice has accumulated on the exposed members of the structure due to low temperature and/or precipitation (e.g. snow) [1-3]. Under this perspective, the development of a framework for performance based assessment [4] for lattice steel structures used in telecommunication or power transmission networks is essential. The first step towards this effort is the estimation of the fragility of those structures under weather hazards and especially wind and icing conditions [5].

The most critical part for a performance based analysis of steel lattice structures requires detailed and precise calculations of the wind forces acting on the structure. Methodologies for estimation of wind force at lattice structures proposed by current standards (e.g. EN1991-1-4) are mainly based on the solidity ratio of the structure. In cases of a telecommunication tower carrying microwave dish antennas, the shielding effects of the antennas should be taken into account. However, due to the lack of sound guidelines in standards, the estimation of the shielding effects is usually based on wind tunnel tests [6-8].

Considering the above, the purpose of this paper is to present a case study of a telecommunication tower carrying four microwave dish antennas, and designed for coastal areas of Greece according to European standards [9]. The ultimate goal is the estimation of the structure's fragility under possible combinations of wind speed and icing conditions. For this reason, a 3D model was developed in open-source software and a 3D simulation of the wind field was conducted capturing the spatial and temporal variation of wind speed over the entire profile of the structure. Moreover, the impact of ice was assessed by considering a range of various uniformly thick layers of accumulated ice on the exposed tower members and dishes. The estimation of the fragility was based on the processing of the results of a large number of non-linear dynamic analyses via probabilistic methods.

The results could be elaborated for performance-based design and analysis of telecommunication towers. Furthermore, if the fragilities are used in combination with climatic data from the site of installation a risk assessment of this particular type of structure would be possible. This assessment could be valuable to telecommunication companies as a useful decision support tool regarding their needs to replace or upgrade their existing tower network.

2 TOWER MODEL

2.1 Geometry

The main body of the lattice tower of the study is 48 meters tall and has a square cross section [9]. At the top of the tower though, a pyramid that holds the lightning rod is formed and ends at a height of 51m. A complete view of the tower is presented in Figure 1a. The view of the tower can be divided into two main sections. The first section is an inclined one, whose

square cross section reduces with height and runs from 0 to 24m. The second section is a vertical one, which runs from 24 to 48m and has no inclination since it is designed to carry the antennas. The tower has horizontal diaphragms every 3 meters along its height (Figure 1b). It also includes five working platforms at heights of 12, 24, 42 and 45m (Figure 1c). Finally, a ladder and a waveguide rack for the cables of the antennas run connecting the centers of the horizontal diaphragms.

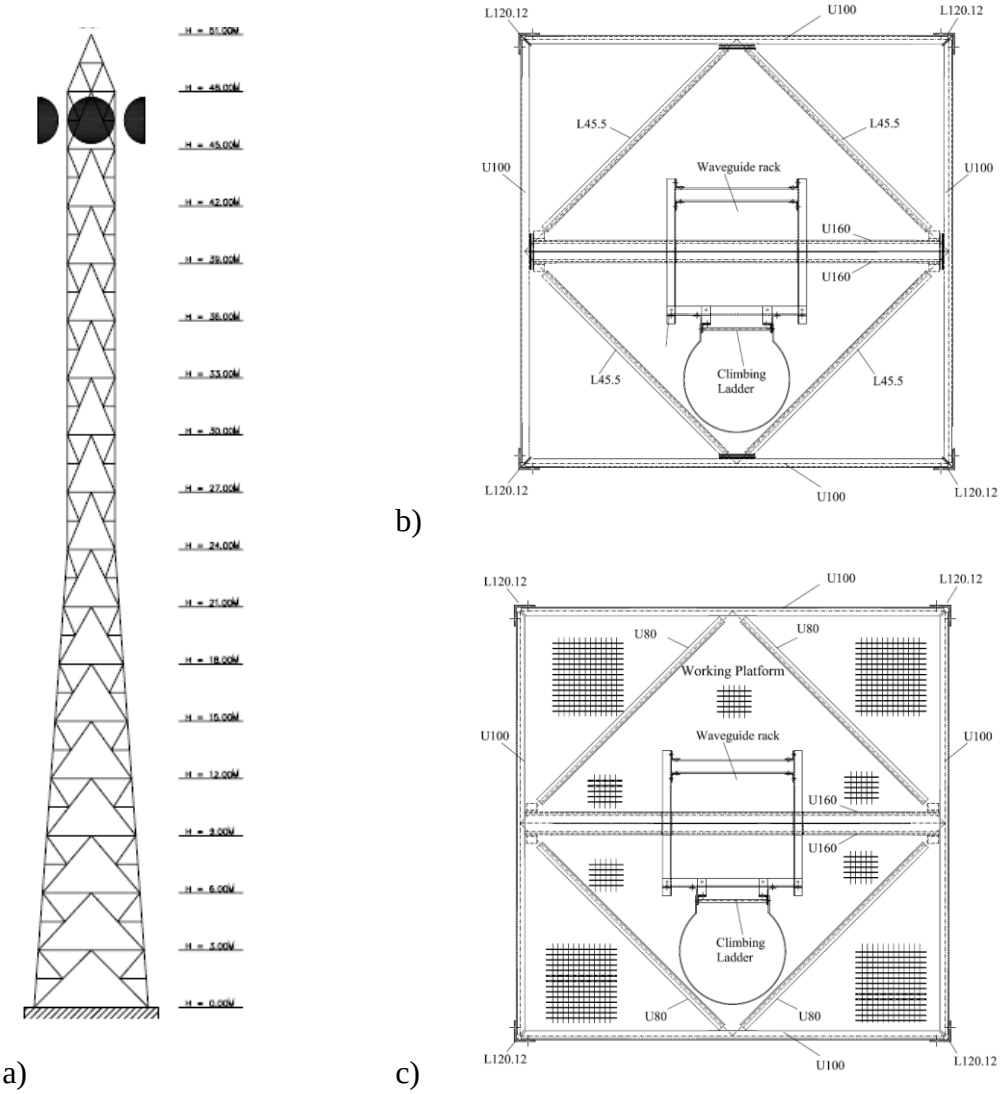

Figure 1: a) Complete view of the tower. b) Typical plan of a horizontal diaphragm. c) Typical plan of a working platform [9].

The structural members of the tower consist of channel and angle steel sections. The members could be characterized as (Figure 2): legs, (main) vertical diagonals/bracing members, secondary vertical bracing members, horizontals, horizontal diagonals and a central horizontal member at each diaphragm which carries the loads of the ladder, the waveguide rack and the cables.

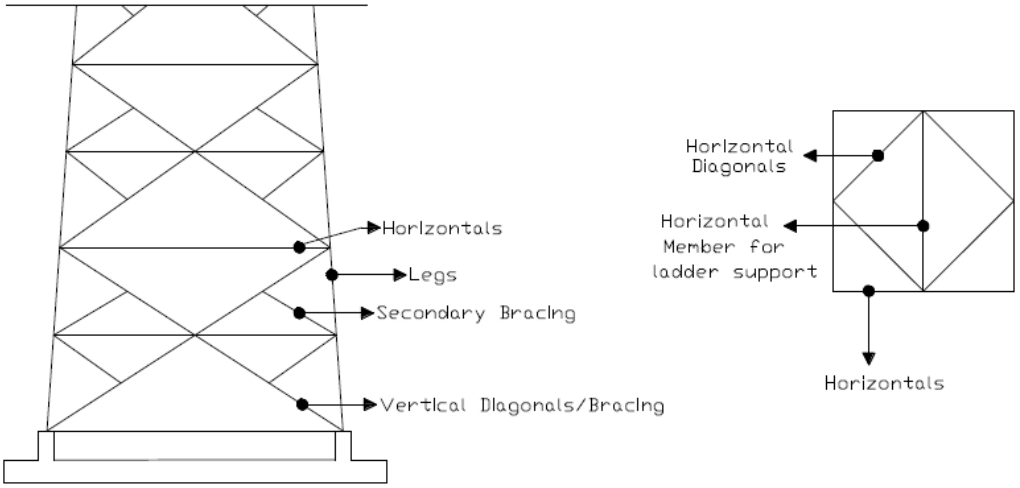

Figure 2: Designation of structural members [9].

As far as the legs are concerned, two types of angle sections were used. Specifically, the legs of the inclined section (height: 0-24m) were constructed from L160.15, while the legs of the vertical section (height: 24-48m) were constructed from L120.12. For the main vertical diagonals, an angle L70.7 section was used throughout the whole height of the structure, while for the secondary vertical diagonals a L45.5 section was used. The horizontal members of each diaphragm were constructed from a channel U100 section. For the horizontal diagonal members an angle L45.5 was used, except for the five levels of the working platforms where a channel U80 section was employed. On the other hand, the central horizontal member of each diaphragm was formed by 2 channel U160 sections welded on both edges. Finally, the members of the pyramid at the top of the tower (height: 48-51m) were made by L70.7.

2.2 Material

The structural steel grade was S355J2K2 for legs and S235J0JR for the rest of the members. At this point it should be noted that since the purpose of this work is not the design but a performance assessment for a lattice telecommunication tower, the real values of steel strength (as estimated by experimental work listed in the literature) were assumed in the analysis, instead of the nominal ones. Specifically, for steel grade S355J2K2, the (mean) yield strength f_y is equal to 454.90 MPa and the (mean) tensile strength f_u is equal to 546.84 MPa. On the other hand, for S235J0JR the corresponding values are 328.80 MPa and 435.41MPa, respectively [10]. The material stress-strain curve that was assumed in the analysis is presented in Figure 3. The value of E corresponds to steel Young's Modulus and is equal to 210 GPa, while the the buckling reduction factor χ was calculated for each structural member according to EN 1993-1-1 [11] to reduce its compression strength. Since the members of the tower have different properties according to their cross-section, the stress-strain curve is different for each member and thus Figure 3 presents only the general form of the stress-strain curve for all members.

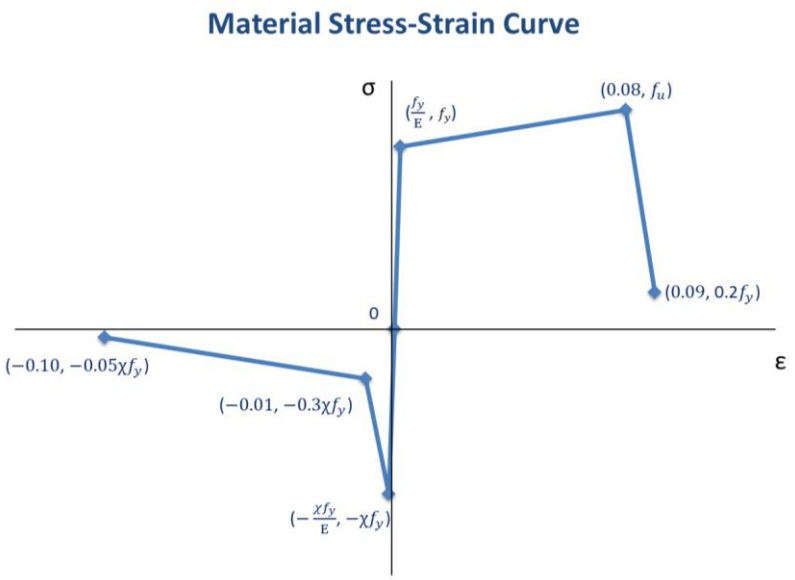

Figure 3: General form of a member stress-strain curve

2.3 Loads

2.3.1 Gravity loads

The unit weight of steel is equal to 78.50 kN/m^3. The weight of the climbing ladder is 15.30 kN and the weight of waveguide rack 14.60 kN. Four dish antennas are installed at the top (height 45-48m) of the tower. Each dish antenna has a weight of 2.30 kN. The weight of the cables is assumed to be 0.05 kN/m per dish. Finally, the weight of the five working platforms is 0.25 kN/m^2.The live load of the climbing ladder is 5.00 kN, while the live load at the working platforms is assumed to be 2.00 kN/m^2.

2.3.2 Wind loads

In the case of a telecommunication tower with dish antennas, the total wind force acting on the structure consists of two main components, namely the force acting on the tower (i.e. the structural members) and the force acting on the dish antennas [6,8,12]:

$$F_T = F_{tower} + F_{antennas} \quad (1)$$

Wind Force at the tower

The wind force acting on the tower is calculated by the Equation:

$$F_{tower} = qC_DA_{ref} \quad (2)$$

where: q is the dynamic pressure of the wind, C_D is the drag coefficient and A_{ref} is the area of the members projected normal to the level of the wind.

The dynamic pressure of the wind q depends on the air density ρ and the wind speed u and is estimated using the following Equation:

$$q = \frac{1}{2}\rho u^2 \quad (3)$$

Herein, ρ was assumed to be equal to 1.225 kg/m^3.

The drag coefficient C_D for lattice steel structures depends on the solidity ratio φ. According to EN1991-1-4 [13], the solidity ratio φ is the fraction of the sum of the projected area A

of the members of the structure's face normal to that face divided by the total enclosed area A_c by the face's boundaries projected normal to that face. Thus:

$$\varphi = \frac{A}{A_c} \tag{4}$$

In this work, the structure was divided into sixteen segments (every 3 m) along its height considering each horizontal diaphragm to be at the middle of the segment. For each segment the solidity ratio was calculated and the corresponding drag coefficient was estimated based on [13]. Finally, the forces of each segment were assigned to the level of the corresponding diaphragm.

Wind Force at the dish antennas

According to [12], the commonly used practice in the past for the estimation of the wind force on dish antennas was to calculate the drag coefficient of the isolated antenna, then the corresponding force, and finally adding the result to the force of the tower as calculated by Eq. (2). However, this practice would overestimate the total force since the antenna may shield part of the tower. This is also evident in case of multiple antennas installed on the tower. For this reason, except for the drag coefficient of the isolated antenna, an additional interference factor should be added in the estimation. Thus the wind force, in case of two identical in size antennas installed on the same height at the tower, is calculated as follows [6, 8]:

$$F_{antennas} = qA_a(C_{Da_1}f_{a_1} + C_{Da_2}f_{a_2}) \tag{5}$$

where: q is the dynamic pressure of the wind, A_α is the area of each antenna projected normal to the level of the wind, $C_{D\alpha 1}$ and $C_{D\alpha 2}$ are the drag coefficients for the two isolated antennas and $f_{\alpha 1}$ and $f_{\alpha 2}$ are the corresponding interference factors for each of the antennas.

The values of the drag coefficients and the interference factors of the antennas are mainly based on the wind angle and the solidity ratio. Those values are usually estimated experimentally [6-8]. Herein, in lack of experimental results for the tower and the antennas, proposed values by an experimental study of a similar case [8] for $C_{D\alpha 1}$, $C_{D\alpha 2}$, $f_{\alpha 1}$ and $f_{\alpha 2}$ were adopted.

2.3.3 Ice Loads

Apart from wind, another environmental hazard that should be taken into account is ice. In the case of a lattice telecommunication tower, ice accumulates on the surface of the structural members and the dish antennas. Ice accretion affects the loads of the structure in two major ways. First, the weight (i.e. dead load) of the members and the dish antennas increase and secondly, the projected area of the members and the antennas also increase. Following the previous section, where the estimation of the wind loads was discussed, it can be inferred that an increase in the projected area of the members affects the solidity ratio of the tower and the corresponding drag coefficients resulting in a larger wind force for the same wind speed value.

In this work, it was assumed that an ice layer of uniform thickness was formed on the surface of the exposed parts of the members and the dish antennas. In terms of the value of the ice thickness, three scenarios of different values were considered, namely 15mm, 30mm and 45mm. For each of those icing scenarios, the corresponding areas of the ice surface and the associated values of the affected parameters (e.g. weight, solidity ratio etc.) were estimated. Finally, it should be noted that the unit weight of ice was considered equal to 7.00 kN/m^3.

3 ANALYSIS

3.1 OpenSees model

For the analysis, the tower was modeled in OpenSees, an open-source software, provided by Pacific Earthquake Engineering (PEER) Center [14]. The final 3D model (Figure 3) was composed by 932 members, both trusses and beams. The members were also modeled as fiber sections sharing the same properties of the corresponding steel cross-sections used in the structure. In total, four different versions were analyzed, one for no icing conditions and one for each of the three different scenarios of ice thickness as presented in a previous section.

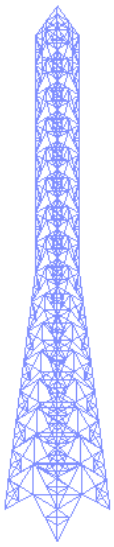

Figure 3: 3D model created in OpenSees.

The natural frequencies of the structure were determined by a modal analysis. The first two modes have the same period due to structure's and loads symmetry, although refer to different directions (X and Y). The third mode is torsional.

Modal analyses were also performed for each of the icing scenarios. Table 1 presents the periods of the first three modes for each scenario. The results show, as expected, that as the thickness of the ice layer increases, the corresponding periods increase. Certainly, this should be attributed to the increase of the tower (and dish antennas) mass.

Ice Thickness (mm)	T_1 (sec)	T_2 (sec)	T_3 (sec)
15	0.901	0.901	0.305
30	1.108	1.108	0.370
45	1.316	1.316	0.436

Table 1: Natural periods of the first three modes for the three icing scenarios considered.

3.2 Wind speed simulation

3.2.1 Wind speed profile

Wind speed increases with height following a specific pattern known as wind speed profile. Herein, a power law wind speed profile was considered. According to the power law profile, the value of wind speed at a height z is given by:

$$\frac{u}{u_{ref}} = \left(\frac{z}{z_{ref}}\right)^{a} \tag{6}$$

where: u is the wind speed at height z (in m/s), u_{ref} is the wind speed at a reference height z_{ref} (in m/s) and α is the power law exponent. In this work, a power law exponent α=0.20 was used, as proposed by IEC 61400-1 [15] for onshore structures. Eq. (6) gives the values of the wind speed along the height of the tower. Herein, the values of wind speed at the heights of the horizontal diaphragms and the center of the dish antennas were calculated. Based on these values, the wind force along the height of the tower is estimated by applying Eq. (1) and Eq. (2).

3.2.2 Wind field simulation

The simulation of the wind field where the tower is placed was performed in TurbSim software [16]. TurbSim has been developed by National Renewable Energy Laboratory of the USA and is mainly used in wind industry applications. The software simulates a 3D wind field. TurbSim can also generate timeseries of wind speed over a user-defined period (e.g. 10 min, 1 hour etc.) and for a specific wind speed value which is considered to be the mean wind speed (reference wind speed). The wind field is defined by a custom grid whose dimensions and resolution are specified by the user. The software finally outputs the corresponding timeseries of the values of the three wind speed components (for each of the three directions X, Y, Z) at the points of the grid of the wind field. For each of those components the corresponding wind force timeseries (mainly for the directions X and Y, since the component of direction Z is ignored in this study) were estimated by applying Eq. (2) for the wind force at the tower and Eq. (5) for the wind force at the antennas.

3.3 Pushover analysis

As a first step before the nonlinear dynamic analysis, a pushover (nonlinear static) analysis was performed in order to specify the failure mechanisms of the tower. The lateral load profile considered in the pushover was following the pattern of the wind force. Pushover analysis was conducted for no ice conditions and the three scenarios of icing. In all cases, the failure mechanism revealed a cascading effect shown in Figure 4. It is evident that the first member failure occurs at the point of the tower where the inclination of the legs changes to vertical, a change which also coincides with the change in the legs' cross-section from L160.15 to L120.12. The first element that fails could be either a leg or a main vertical bracing member (marked with a red circle in the figure). As lateral loads increase, the failure cascades to other elements resulting finally in a total collapse.

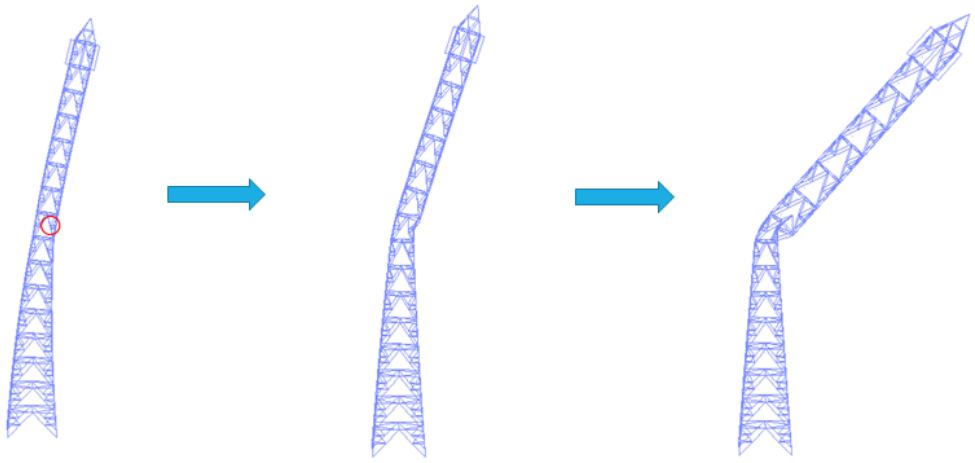

Figure 4: Failure mechanism as revealed by pushover analysis

Figure 5 presents the pushover curves for each of the four versions of tower (no ice and icing scenarios). The horizontal axis depicts the displacement of the top of the tower along the lateral loads direction, while the vertical axis depicts the shear force at the base of the tower. The curves show that the maximum shear force (i.e. the shear force when the first failure occurs) is approximately the same for the four versions and close to 470 kN. The corresponding displacement of the top (height 51m) at the time of the first failure is approximately 0.68 m in all versions.

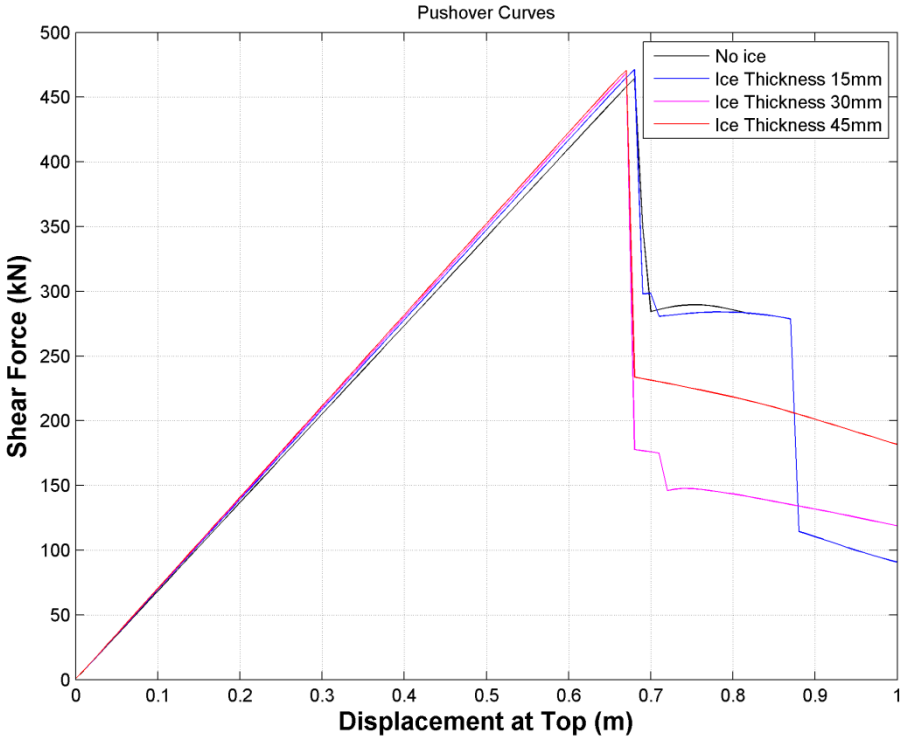

Figure 5: Pushover curves for each of the four versions of ice thickness considered.

3.4 Dynamic analysis

The main input for the nonlinear dynamic analysis was the timeseries of the wind speed created in TurbSim software as discussed above. Thus, the wind speed value (i.e. the wind speed profile) was estimated for specific points at the heights of the horizontal diaphragms of the tower. Figure 6 presents a typical form of the wind speed timeseries at the level of the top horizontal diaphragm (height 48m). The length of the timeseries was 1 hour (3600 seconds).

The next step of the analysis was to estimate the timeseries of wind force along the height of the tower (i.e. the wind force profile). The estimation was done by processing the results of the timeseries of wind speed and performing the necessary calculations by applying Eq. (1) along the two horizontal directions (X and Y). Thus, the wind force profile for the two horizontal directions was created. Those values constituted the inputs of the dynamic parameters for the OpenSees software where the dynamic analysis was performed.

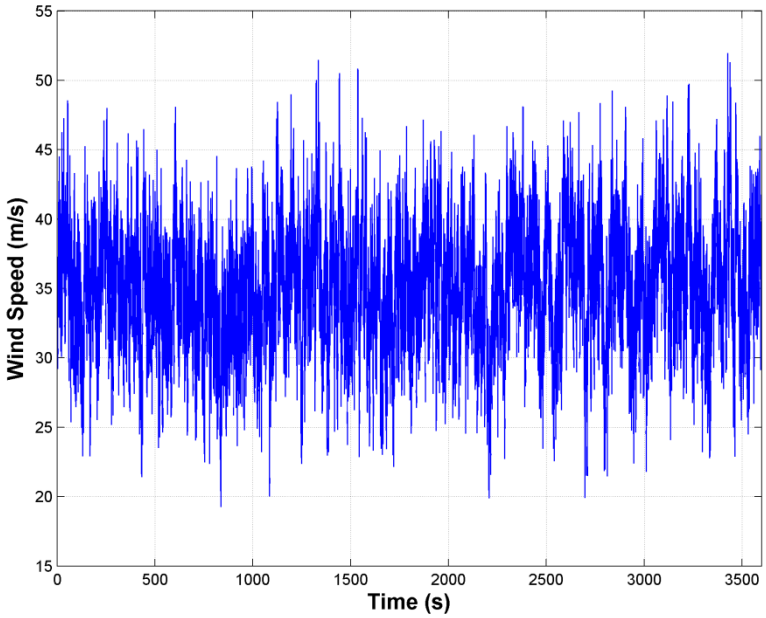

Figure 6: Typical form of 1hr wind speed timeseries (reference wind speed 35 m/s).

In an attempt to reduce computational effort and time, only five different values for wind speed with a horizontal angle of 0 degrees (i.e. parallel to X axis) were considered, namely 20, 25, 30, 35 and 40 m/s. Those values were actually the reference values of wind speed (constituting the inputs for TurbSim software) and their height was the height of the top horizontal diaphragm (height 48m). Moreover, for each of the above values, six timeseries were created resulting in a total of 5×6=30 different timeseries of wind speed. Consequently, 30 different wind dynamic analyses were performed in OpenSees software for each of the four tower versions (no ice conditions and the three icing scenarios) considered in this work. Finally, it should be noted that the same 30 timeseries of wind speed were used for the four versions in order the final results to be comparable. However, the resulting wind force timeseries were different since wind force is affected by ice thickness.

3.5 Fragility analysis

The ultimate goal of this work was to estimate the fragility of the tower to wind and/or icing conditions. Fragility could be defined as the probability of failure for a given intensity measure (*IM*), herein the value of wind speed. The results of such an analysis are reported in the form of fragility curves. The estimation of the fragility functions and corresponding curves is based on the probability of failure for the various values of the *IM*, i.e. the wind speed in this case. A common assumption is that the fragility curve is defined by a lognormal cumulative function (CDF) with the following mathematical expression [17]:

$$P(C|IM = x) = \Phi\left(\frac{ln(x/\theta)}{\beta}\right) \tag{7}$$

where: $P(C|IM=x)$ is the probability that a value of the *IM* (e.g. the wind speed) equal to x will cause a failure of the structure, $\Phi(\ )$ is the standard normal cumulative distribution function (CDF), θ is the median of the fragility function which corresponds to the value of *IM* with 50% probability of failure and β is the standard deviation of *lnIM*, sometimes referred to as dispersion of *IM*.

A simple method to estimate fragility is by performing stripe analysis. Stripe analysis is mainly applied when discrete values of *IM* are used, as in the case of this work. The first step of the process is to perform a number of dynamic analyses for each value of the *IM*, namely the wind speed, and then estimate the number of cases where a failure was occurred. Then for each wind speed the fraction of analyses causing failure could be estimated by simply dividing by the total number of analyses. This fraction is actually an estimator of the probability of failure for the corresponding value of the *IM*.

In this work, six dynamic analyses were performed for each of the five different reference values of wind speed based on the wind speed timeseries discussed in a previous section and for each of the four versions of tower considered. Finally, a failure was assumed that occurs in two ways. First, when the mean value of the inter-story drift during the first 10 minutes of the analysis is different from the corresponding mean value of the last 10 minutes of the analysis. Secondly, if the dynamic analysis was failed (i.e. it was incomplete) due to non-convergence of the algorithm used by the OpenSees software.

Figure 7 shows the stripe analysis results for no ice conditions. A blue circle denotes a non-failure result of the dynamic analysis. A red triangle denotes a failure result of a converged dynamic analysis, while a black asterisk denotes a non-converged dynamic analysis. Following the results of Figure 7, the estimation of the probability of failure for each combination of wind speed and ice thickness can be estimated by simply calculating the fraction of analyses causing failure, as presented in Table 2.

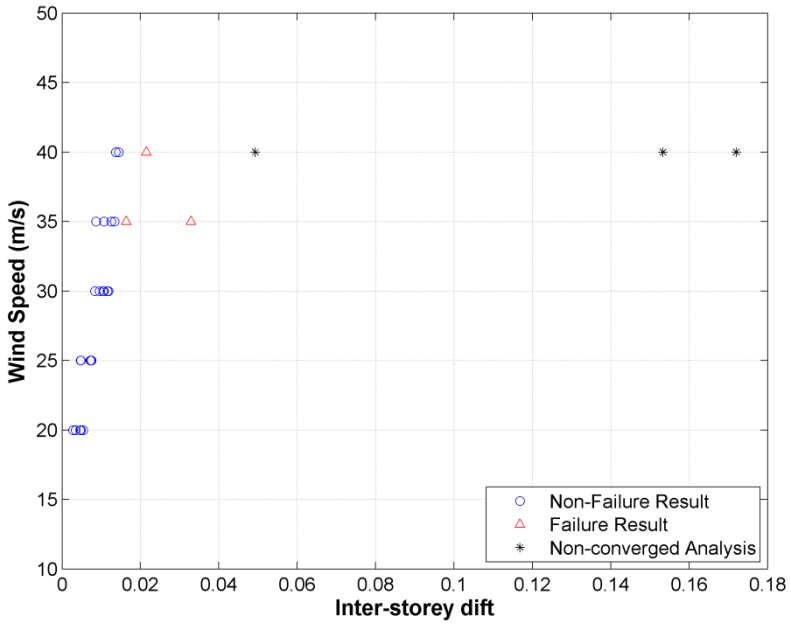

Figure 7: Stripe analysis for no ice conditions.

Wind Speed (m/s)	No Ice	Ice thickness 15 mm	Ice thickness 30 mm	Ice thickness 45 mm
20	0.00	0.00	0.00	0.00
25	0.00	0.00	0.00	0.17
30	0.00	0.33	0.50	0.33
35	0.33	0.67	0.67	1.00
40	0.67	1.00	1.00	1.00

Table 2: Fraction of analyses causing failure for combinations of wind speed and ice thickness

The next step is to fit a lognormal cumulative function (Eq. (7)) to the values listed in Table 2. The parameters θ and β can be easily estimated by maximum likelihood estimation method as in [17].

Results show that for no ice conditions, the median wind speed (θ) of the fragility function is 37.62 m/s. On the other hand, for ice thicknesses of 15mm, 30mm and 45mm, the corresponding values are 32.28 m/s, 31.48 m/s and 29.55 m/s, respectively. This means that as ice accumulates on the tower, the median wind speed of failure decreases. At the same time, the probability of failure increases, as the thickness of the ice layer increases. The last is also evident if the four fragility curves are plotted on the same graph as in Figure 8. It is obvious that the position of the fragility curve moves to the left as ice thickness increases. This finding should be attributed to the impact that ice has on the structure by increasing both the dead loads and the wind force for the same wind speed.

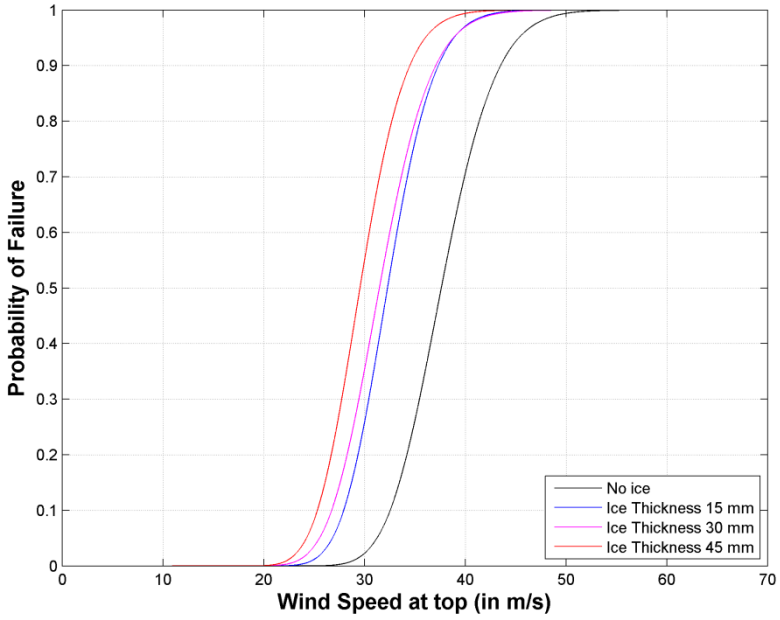

Figure 8: Fragility curves for wind speed and ice thickness combinations

4 CONCLUSIONS

Telecommunication towers are tall steel lattice structures vulnerable to weather hazards. In this paper, a case study of a telecommunication tower carrying four dish antennas and designed for coastal areas of Greece was presented. For the analysis of the tower a 3D model was developed in an open-source software.

A number of nonlinear dynamic analyses of the 3D model of the tower were performed in order to estimate the fragility of the tower to wind and icing conditions. For those analyses, timeseries of wind speed and corresponding force at the structure were created based on a detailed 3D simulation of the wind field along the entire profile of the tower. Furthermore, four different cases of icing conditions were examined by developing the corresponding models. Finally, the fragility of the structure for every combination of wind and icing conditions was estimated and the corresponding fragility curves were created following a probabilistic methodology.

The results confirm the significant effect of wind on steel lattice structures, especially when it is combined with ice accretion. Specifically, the probability of failure (and probably collapse) tends to increase as ice accumulates on the structure for the same wind speed value in comparison with no ice conditions. This finding is in accordance with related literature.

At the end, the elaboration of climatic data from the site of the structure could be proposed as an extension of this work. Based on climatic data, the probabilities of occurrence of all wind and icing combinations over a specified period (e.g. service life of structure) could be estimated. By incorporating these probabilities along with the fragility curves presented herein, one could estimate the risk of the structure over its projected lifetime. This risk estimation could be used as a useful decision tool by telecommunication companies in upgrading and/or expanding their network.

ACKNOWLEDGMENTS

This research has been financed by the European Commission (Research Program of the Research Fund for Coal and Steel) through the Program "ANGELHY - Innovative solutions for design and strengthening of telecommunications and transmission lattice towers using large angles from high strength steel and hybrid techniques of angles with FRP strips" with Grant Agreement Number: 753993.

REFERENCES

[1] C. Klinger, M. Mehianpour, D. Klingbeil, D. Bettge, R. Hacker, W. Baer, Failure analysis on collapsed towers of overhead electrical lines in the region Münsterland (Germany) 2005, *Engineering Failure Analysis*, **18**, 1873-1883, 2011.

[2] L. Makkonen, P. Lehtonen, M. Hirviniemi, Determining ice loads for tower structure design, *Engineering Structures*, **74**, 229-232, 2014.

[3] D.K. Davis, North American tower failures: causes and cures. *Consolidated Engineering Inc*, 2010.

[4] Y. Wang, D.V. Rosowsky, Characterization of joint wind-snow hazard for performance-based design, *Structural Safety*, **43**, 21-27, 2013.

[5] S.N. Rezaei, Fragility assessment and reliability analysis of transmission lines subjected to climatic hazards, *PhD Dissertation*, McGill University, Monteal, Quebec, Canada, 2016.

[6] J.D. Holmes, R.W. Banks, G. Roberts, Drag and aerodynamic interference on microwave dish antennas and their supporting towers, *Journal of Wind Engineering and Industrial Aerodynamics*, **50**, 263-270, 1993.

[7] C.F. Carril Jr, N. Isyumov, R.M.L.R.F. Brasil, Experimental study of the wind forces on rectangular latticed communication towers with antennas, *Journal of Wind Engineering and Industrial Aerodynamics*, **91**, 1007-1022, 2003.

[8] P. Martin, V.B. Elena, A.M. Loredo-Souza, E.B. Camano, Experimental study of the effects of dish antennas on the wind loading of telecommunication towers, *Journal of Wind Engineering and Industrial Aerodynamics*, **149**, 40-47, 2016.

[9] ANGELHY Deliverable 1.3, Report on analysis and design of 6 case studies, *Research Program of the Research Fund for Coal and Steel ANGELHY, Grant Agreement Number: 753993*, European Commission, Brussels, Belgium, 2019.

[10] A. Braconi et al. Optimising the seismic performance of steel and steel-concrete structures by standardising material quality control (OPUS), *Research Program of the Research Fund for Coal and Steel ANGELHY, Grant Agreement Number: RFSR-CT-2007-00039*, European Commission, Brussels, Belgium, 2013.

[11] EN 1993-1-1, Design of steel structures. Part 1-1: General rules and rules for buildings. Brussels. Comité Européen de Normalisation (CEN), 2005.

[12] J.D. Holmes, *Wind loading of structures, Third Edition*, CRC Press, Taylor & Francis Group, 2015.

[13] EN 1991-1-4, Design of steel structures. Part 1-4: General actions – Wind actions. Brussels. Comité Européen de Normalisation (CEN), 2005.

[14] S. Mazzoni, F. McKenna, M. Scott, G. Fenves, Open system for earthquake engineering simulation. User Command-Language Manual, Report NEES grid-TR 2004-21, Berkeley, CA: Pacific Earthquake Engineering Research, University of California, 2006. Retrieved http://opensees.berkeley.edu

[15] IEC 61400-1. "Wind Turbines-Part 1: Design Requirements," International Electrotechnical Commission, Geneva, Switzerland, 2005.

[16] B.J. Jonkman, L. Kilcher, TurbSim User's Guide. Technical Report NREL/TP-xxx-xxxx (Draft Version). NREL Technical Report, National Renewable Energy Laboratory, Golden, Colorado, 2012.
[17] J.W. Baker, Efficient analytical fragility function fitting using dynamic structural analysis, *Earthquake Spectra*, **31**, 579-599, 2015.